ACS OMEGA

http://pubs.acs.org/journal/acsodf

Article

Simultaneous Enhancement of Polymerization Kinetics and Properties of Phthalonitrile Using Alumina Fillers

Yu Shan Tay,[†] Eric Jian Rong Phua,[†] Zhong Chen, and Chee Lip Gan*

Cite This: *ACS Omega* 2022, 7, 32996−33003

Read Online

ACCESS | Metrics & More | Article Recommendations | Supporting Information

ABSTRACT: Alumina particles are investigated as a potential catalyst for phthalonitrile polymerization and as a property enhancer. In this work, extensive characterizations were conducted on alumina-filled resorcinol-based phthalonitrile to differentiate between the catalytic effect and the filler effect. Thermal gravimetric analysis (TGA) and Fourier transform infrared (FTIR) spectroscopy suggest the occurrence of chemical interaction between alumina fillers and phthalonitrile, which provides an insight into the better performance of alumina-filled phthalonitrile resins. This hypothesis is further supported by the additional Al−N peak observed in the X-ray photoelectron spectroscopy (XPS) analysis when alumina is added to phthalonitrile before curing, as well as the presence of an exothermic peak in the differential scanning calorimetry (DSC) analysis that indicates the catalytic polymerization of phthalonitrile. This catalytic phenomenon observed by the addition of alumina fillers is beneficial for the improvement of the conventionally slow curing process of phthalonitrile and, more importantly, is coupled with observable enhancement of thermomechanical properties of the composite.

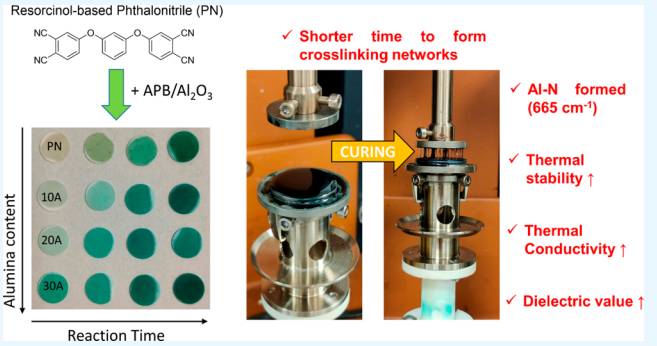

INTRODUCTION

In the past few years, phthalonitrile (PN) polymer research has been increasing rapidly, with consistent focus on material improvisations to overcome its intrinsic shortcomings. It is known that phthalonitrile resins have superior properties, such as a high operating temperature, over traditional high-performance polymers such as polyimide and cyanate esters, but its curing process can be sluggish and requires high temperature treatment. Various solutions have been introduced such as modification of the chemical structure of the phthalonitrile monomer to achieve a lower melting point for lower temperature processability,[1] incorporation of amine groups to allow self-catalytic polymerization,[2] and use of different types of catalyst or curing agents like metals/metallic salts, organic amine, and strong organic acid/amine salts to catalyze the polymerization process.[3]

Separately, phthalonitrile resins are well-blended with other polymers or reinforced with various types of fillers to achieve better thermomechanical properties. Ceramic fillers generally exhibit high strength, high modulus, superior hardness, improved wear properties, low dielectric constant, and high operating temperature.[4,5] They are known to improve the thermomechanical properties of high performance polymers and other application related properties such as anticorrosion and UV shielding properties.[5] Research has shown successful reinforcement in phthalonitrile resins with ceramic fillers such as silicon carbide (SiC), silicon nitride (Si_3N_4), silicon oxide (SiO_2), alumina (Al_2O_3), and titanium oxide (TiO_2),[6−8] resulting in phthalonitrile composites with improved mechanical, dielectric, and thermal properties. Surface modifications of ceramic fillers are commonly employed to ensure better integration of the reinforcing phase within the matrices,[5,9] since interfacial interactions are usually the point of failures. Hence, it is important to determine the chemical compatibility between neat fillers and PN polymer.

Studies done on the different sizes of fillers showed that nanocomposites have potentially far superior mechanical properties as compared to polymers reinforced with microscale fillers.[10] This greater enhancement is achieved due to the increase in surface area for a given volume fraction of the polymer matrices. Moreover, the addition of ceramic fillers to phthalonitrile resins are mainly related to a corresponding change in thermomechanical properties; its effect on the curing behavior remains unclear.

Existing research shows that incorporation of inorganic particles into the phthalonitrile resins has no effect on the

Received: April 29, 2022
Accepted: August 26, 2022
Published: September 7, 2022

Scheme 1. Synthesis of Resorcinol-Based Phthalonitrile

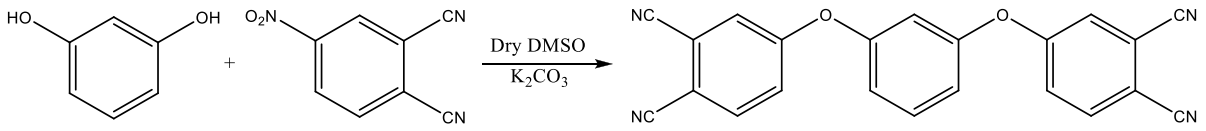

curing temperatures in the presence of curing agent.[5] The addition of silicon nitride[11] and silica nanoparticles[12] did not alter the curing temperature of similar long chain heterocyclic chemical compounds known as polybenzoxazine. A similar trend was also observed in the curing behavior of phthalonitrile resin filled with silicon carbide microparticles.[6] Alumina nanoparticles, when added as a reinforcement in bisphenol-A based phthalonitrile with the presence of self-catalyzing functional group, did not enhance or catalyze the curing kinetics of the polymeric matrix.[8] However, a decrease in the heat polymerization of the alumina-filled nanocomposite was observed and the plausible explanation given was the increase in viscosity due to presence of nanoalumina.[8] As compared to the negligible changes in curing behavior when silica nanoparticles were added, this result is indicative of the possibility of alumina having some catalytic polymerization effect that may be negligible in the presence of a catalyst or self-catalyzing functional groups in the polymer chain.

Polymeric forms of phthalonitrile include poly(triazine), poly(phthalocyanine), and poly(isoindoline). To date, research has not been able to quantify the exact amount of triazine, phthalocyanine, and isoindoline components formed at each stage of curing, primarily due to equipment limitations at high temperature. Hence, it is even more challenging to determine any chemical interaction between fillers and phthalonitrile resins that can be the key influence to enhanced properties in the composites. In previous work,[13] the discrete Fourier transform (DFT) model had been employed to study the possibility and feasibility of bond formation between fillers and polymer matrix to explain the potential cause of matrix failure under stress. Fillers such as alumina and silica were used for the DFT calculations, together with the polymeric forms of resorcinol-based PN. Based on the DFT results, both poly(triazine) and poly(phthalocyanine) form covalent bonds with alumina and silica fillers. However, compared with the calculated enthalpy of formation, the formation of alumina adduct is more favorable.

In this work, experiments were conducted to verify the bond formation between alumina fillers and PN matrix. No surface modification was done on the fillers, so that the study is focused on the intrinsic interaction between fillers and PN polymer. To our surprise, catalytic polymerization was observed when alumina fillers were added in the absence of catalyst. This is beneficial, as we may potentially solve the slow curing problem of phthalonitrile while improving its thermomechanical properties.

EXPERIMENTAL SECTION

Materials and Sample Preparation. Alumina (Al_2O_3, ~0.1 μm) and silicon dioxide (SiO_2, 0.5−10 μm (approximately 80% between 1 and 5 μm)) particles were purchased from Sigma-Aldrich. Both oxides were first dried in an oven at 120 °C for 2 h before use. Resorcinol-based phthalonitrile monomer (PN) was synthesized (yield ~80%) through nucleophilic displacement of a nitrile-substituent from 4-nitrophthalonitrile by the dialkaline salt generated from resorcinol as shown in Scheme 1. Various weight percentages of oxides were mixed with PN and ground in a mortar to ensure homogeneous mixing. The acronyms 10A, 20A, 30A, 40A, 50A, and 70A refer to PN with the respective weight percentages of alumina added and 10S, 20S, 30S, and 40S are acronyms for those with added silica. Two batches of samples were fabricated, one set with 2.5 mol % 1,4-bis(4-aminophenoxy)benzene (APB) with respect to PN added as a curing additive and the other set without any curing additive. Different weight percentages of filler-filled phthalonitrile samples were melted and cured in a silicone mold at temperatures greater than 200 °C. The samples were then postcured with a stepwise profile to 350 °C[14] in a tube furnace under an inert argon atmosphere.

Characterization. Thermal gravimetric analysis (TGA) was carried out using a Thermogravimetric Analyzer Q500, TA Instruments. Dynamic heating at a heating rate of 10 °C/min to 600 °C was performed to study the thermal stability of PN samples in air (60 mL/min). A JEOL JSM 7600-F field-emission scanning electron microscope (FESEM) was used for morphology examination. Fourier transform infrared (FTIR) spectra from 400 to 4000 cm^{-1} with spectral resolution of 4 cm^{-1} were collected using a PerkinElmer Instruments Spectrum GX FTIR spectrometer to study the chemical interaction between alumina and phthalonitrile. X-ray photoelectron spectroscopy (XPS) measurements were conducted using Kratos AXIS Supra to investigate the chemical bonding present in the samples. TA Instrument Discovery Hybrid Rheometer (HR-3) was used to determine the time taken for cross-linked networks to form in alumina-filled PN without APB. Differential scanning calorimetry (DSC) was used for curing studies of the filler-containing PN systems. Samples were weighed and sealed in hermetic pans. Dynamic heating scans were carried out using Discovery DSC, TA Instruments, from 40 to 380 °C at a heating rate of 10 °C/min under flowing N_2 (40 mL/min).

RESULTS AND DISCUSSION

Chemical Interaction between PN and Alumina. Figure 1 shows the thermal degradation of PN samples with various weight percentages of alumina added. It can be seen that there is an improvement in the thermal stability of the alumina-filled PN as compared to the neat PN. The onset of degradation can be seen to have shifted to a higher temperature when alumina was added. This phenomenon was also observed when silica was added. However, in comparison with alumina-filled samples, the increase in silica-filled samples is limited, as shown in Figure S1.

From the inset table in Figure 1, there is an increase in temperature for the PN samples to degrade by 5% weight loss. An increasing trend of $T_{5\%}$ can be observed with higher alumina loadings. This effect could be attributed to new interactions between alumina fillers and polymer matrix which lead to new bond formation. Higher filler loading leads to

https://doi.org/10.1021/acsomega.2c02667
ACS Omega 2022, 7, 32996−33003

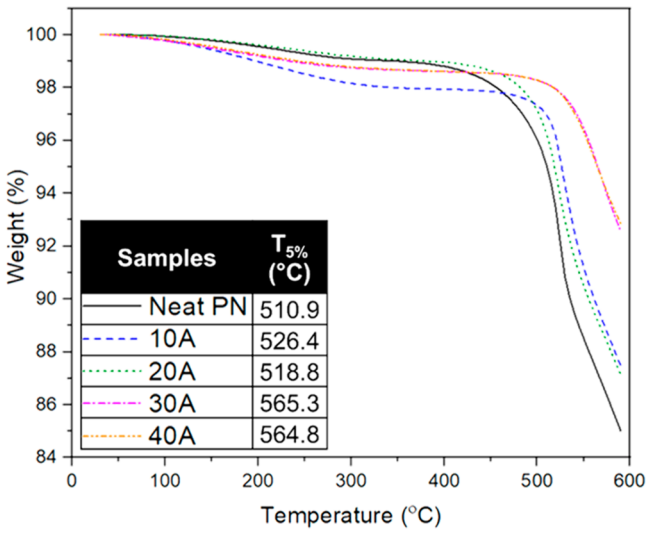

Figure 1. Thermal gravimetric analysis of 0, 10, 20, 30, and 40 wt % alumina-filled PN. Inset table is a summary of $T_{5\%}$ of all the samples.

higher chances of bond formation between PN moieties and the alumina fillers. Figure 1 also shows that the total weight loss decreases with increased weight% of alumina fillers, but this could partially be attributed to a higher weight percent of fillers, which did not degrade over the TGA test temperatures.

Since the addition of oxide fillers to PN samples gives rise to an increase in thermal stability that may suggest possible bond formation between PN and fillers, to further determine any bonding between alumina fillers and PN matrix, we employed FTIR to identify any new bond formation. As above-mentioned, research to date is unable to quantify each of the polymeric forms of PN, but FTIR can still qualitatively identify the presence of each form as shown in Figure 2. In Figure 2a,

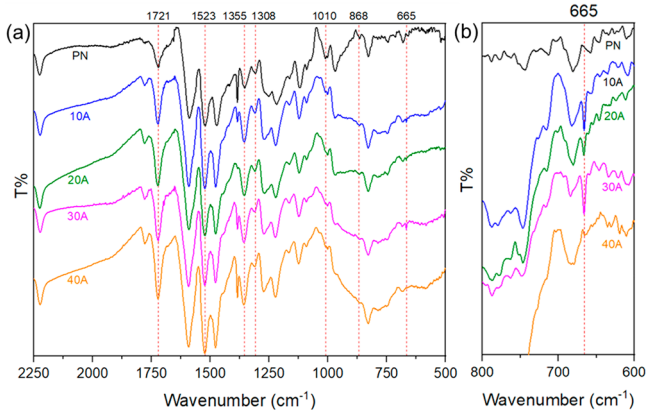

Figure 2. (a) FTIR spectra of 0, 10, 20, 30, and 40 wt % alumina-filled PN samples and (b) enlarged version from 600 to 800 cm^{-1} for better identification of the 665 cm^{-1} peak.

the peak at 1721 cm^{-1} corresponds to that of isoindoline structure[15] and the peaks at 1355 and 1523 cm^{-1} correspond to triazine ring in poly(triazine) structure.[16] The peaks at 868 and 1308 cm^{-1} correspond to metal-free phthalocyanine[17] and a weak characteristic peak at 1010 cm^{-1} corresponds to phthalocyanine,[18] which diminished with an increase in fillers.

For Al−N bond, the adsorption lies between 741 and 755 cm^{-1}.[19] However, in neat PN, there are also peaks appearing within this range, and the Al−N bond would most likely be masked under the characteristic peaks of PN. Also, work done by Vanbuskirk et al.[20] shows that high-purity AlN films give rise to a peak at 665 cm^{-1}. With reference to Figure 2, Al−N bonds are not very infrared (IR) sensitive, and hence it is very challenging to detect the corresponding peaks that will appear less prominent in the FTIR. Figure 2b is an enlarged version of the FTIR spectra for easy identification of the peak at 665 cm^{-1}. Peaks corresponding to 665 cm^{-1} are observed only for the alumina-filled samples and not for the neat PN. This indicates that Al−N bond is present in all the alumina-filled samples. Coupled with the decrease in phthalocyanine characteristic peak with higher alumina loadings, the formation of phthalocyanine-alumina adduct may be less favorable as compared to the other polymeric forms such as triazine. XPS analysis was chosen to further confirm the presence of Al−N since the formation of Al−N bond between alumina filler and the PN matrix cannot be conclusively determined by just one characteristic peak in FTIR.

XPS analysis was done on neat PN and filler-containing PN samples before heat treatment and after postcuring process. Figure S2a shows the chemical structure of PN and its polymeric forms and Figure S2b shows the binding energy of N 1s of neat PN with APB added after the postcuring process. The binding energy at 399.07 eV corresponds to that of the nitrile bond in PN[21] and the peak at 400.39 eV is attributed to that of the triazine bond,[22] which is formed only after polymerization occurs. The polymeric forms of PN shown in Figure S2a have similar carbon−nitrogen bonds among the different chemical structures, hence the binding energy of each carbon−nitrogen bond in the respective chemical structures may be very similar. This makes it difficult to differentiate the carbon−nitrogen bonds from each of the chemical structures. SEM image and XPS analysis of the neat alumina used in this study can be found in Figure S3.

Figure 3 shows the binding energy of Al 2p and N 1s of XPS analysis on the 10 wt % alumina-filled PN before and after the curing process. No binding energy that corresponds to Al−N was observed in Al 2p spectrum as shown in Figure 3a. However, a weak signal was observed in N 1s spectrum as shown in Figure 3b. This may be due to the minute amount of Al−N present that is below the deconvolution limit of Al 2p spectrum since the amount of alumina in this sample is comparatively lower at 10 wt %. The occurrence of binding energy at 74.75 eV (Al 2p) in Figure 3c and the presence of binding energy at 396.69 eV in Figure 3d clearly indicates the presence of Al−N after postcuring. Table 1 summarizes the binding energy of Al−N in Al 2p and N 1s spectra across the various alumina-filled PN samples. It is observed that the binding energy corresponding to Al−N at around 74 eV is consistently detected across all the samples. This confirms the hypothesis that chemical bonding occurs between alumina and PN by Al−N bond formation and that this bond is most likely formed during the heat treatment process.

This result further verifies earlier FTIR analysis which predicted that Al−N bonds are formed between alumina fillers and PN matrix during the curing process. Moreover, a catalytic effect was observed when alumina fillers were added, as shown in Figure 4.

Figure 4a−c shows the N 1s XPS spectra of 30A, 50A, and 70A before heat treatment, obtained from 15 mA emission current of the XPS Al X-ray. Similarly, the XPS spectrum of 10A before heat treatment in Figure 3 was also obtained using a 15 mA emission current. Comparing Figure 3b and Figure

https://doi.org/10.1021/acsomega.2c02667
ACS Omega 2022, 7, 32996−33003

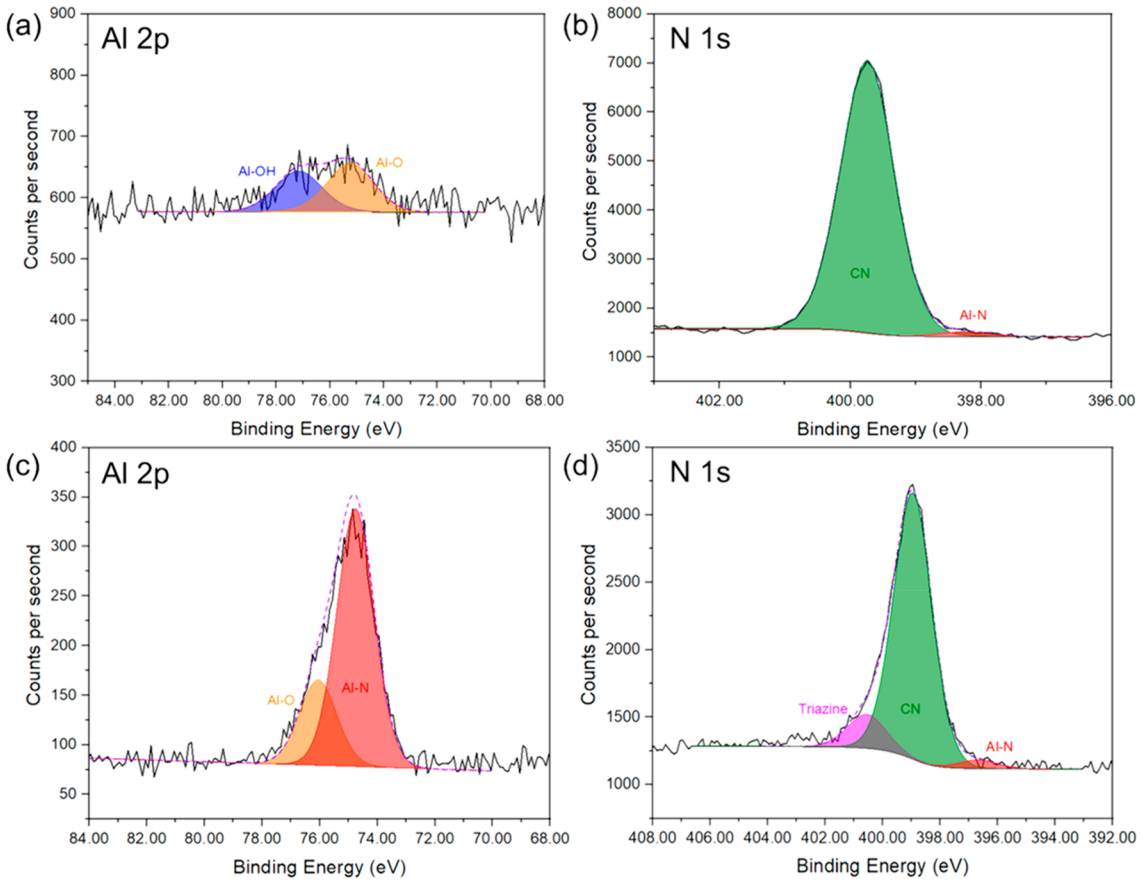

Figure 3. XPS spectra of (a) Al 2p of 10 wt % alumina-filled PN (10A) before heat treatment; (b) N 1s of 10A before heat treatment; (c) Al 2p of postcured 10A; and (d) N 1s of postcured 10A.

Table 1. Summary of Binding Energy Corresponding to Al−OH, Al−O before Heat Treatment and Al−O, Al−N after Postcuring in the Different Alumina-Loaded Samples

	binding engery before heat treatment		binding enegy after postcuring	
samples	Al−OH	Al−O	Al−O	Al−N
10A	77.16	75.24	76.05	74.75
30A	77.59	75.61	75.62	74.60
50A	77.79	75.46	75.30	74.45
70A	77.41	75.40	75.29	74.37

4a−c across samples 10A, 30A, 50A, and 70A, the binding energy that corresponds to the triazine N appears in samples with higher alumina loadings even before heat treatment. Since triazine structure is one of the polymeric forms of PN, this shows that the presence of alumina helps to catalyze the polymerization process. In the absence of alumina or even in the presence of limited alumina content, the triazine ring binding energy would not show up in XPS analysis before any heat treatment is conducted due to its inability to polymerize under ambient condition. The trend across the various alumina-filled PN samples suggests that it is likely to be a two-step process whereby Al−N is first formed before the polymerization of PN takes place as reflected by the Al−N binding energy observed in all 4 samples (15 mA) with the triazine binding energy observed only at higher alumina loadings (Figure 4b, c).

XPS was also carried out with lower emission current of the Al laser at 1 mA (15 W) and 5 mA (75 W) to confirm this hypothesis. Figure 4d, e respectively show the N 1s XPS spectra of 50A and 70A before heat treatment using a 5 mA emission current. Table S1 summarizes the N 1s area ratio of 50A and 70A samples collected with different emission currents for comparison. The 3 N area of interests are triazine N, nitrile N, and Al−N. At lower emission current, Al−N was seen but not triazine. One possible explanation for the formation of Al−N even at lower current is that the Al X-ray source from XPS provides sufficient energy to excite the electrons and promote the formation of Al−N bond between alumina fillers and PN. However, catalytic polymerization of PN is only applicable when a critical quantity of Al−N bond is achieved. Table S1 shows that the formation of triazine is only observed for both samples when an emission current of 15 mA was being employed. This further supports that Al−N is first formed before polymerization takes place, as suggested by the two-step hypothesis.

In comparison, silica-filled PN samples do not exhibit this chemical bonding between filler and polymer, as reflected in the XPS spectra of 30S before heat treatment and after postcuring (Figure S4). No new binding energy corresponding to new bond formation between silica and PN was observed in the XPS analysis of the postcured 30S. The additional binding energy peaks in the Si 2p and O 1s are due to the heat treatment of silica and residue of silicone mold used in the process of PN curing. Therefore, this implies that chemical bonding occurs only between alumina and PN despite DFT simulations suggesting that both alumina and silica adduct are energetically feasible. To further investigate the catalytic effect

https://doi.org/10.1021/acsomega.2c02667
ACS Omega 2022, 7, 32996−33003

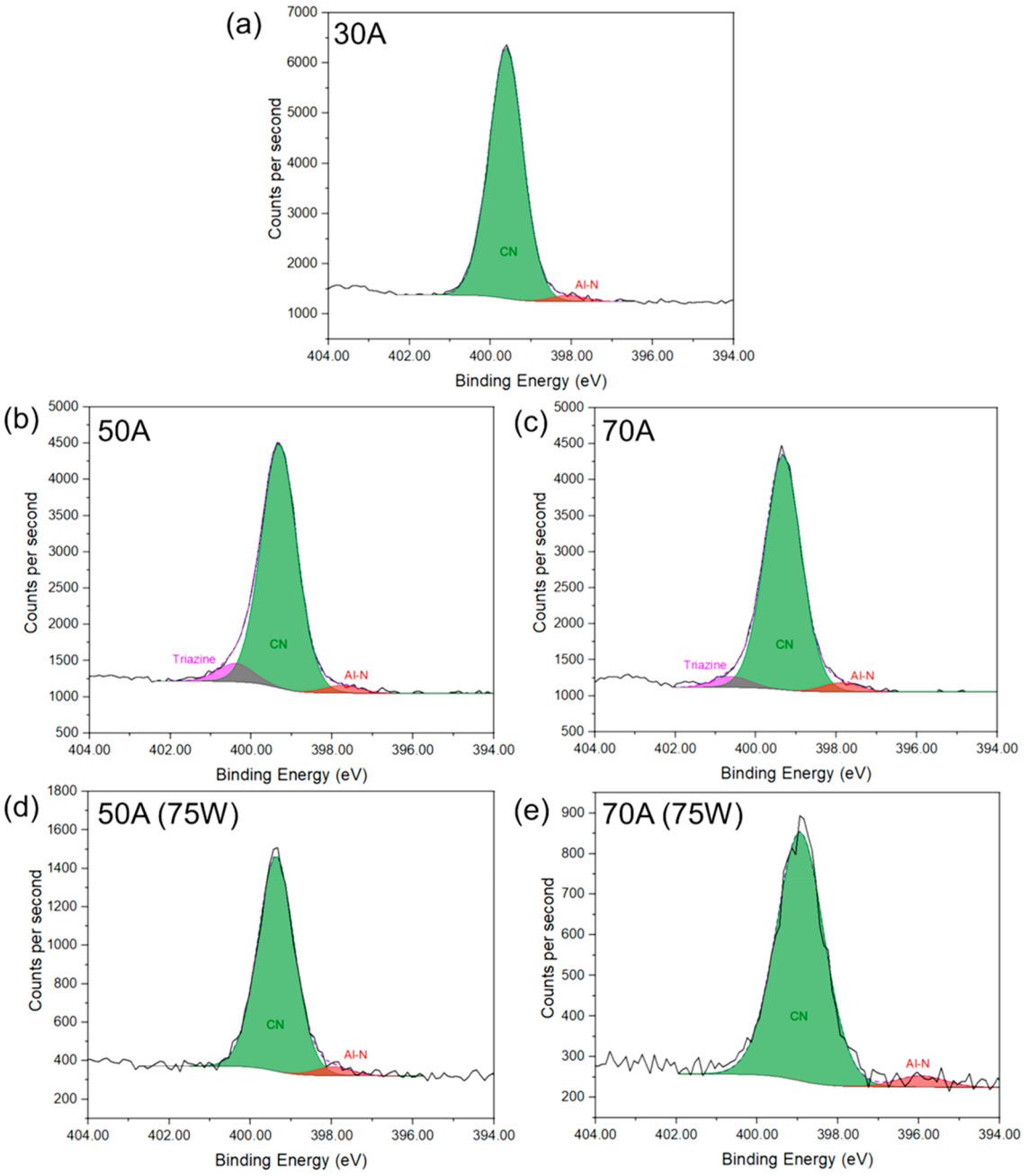

Figure 4. N 1s XPS spectra of (a–c) 30A, 50A, and 70A before heat treatment at a 15 mA emission current (225 W); (d, e) 50A and 70A before heat treatment at a 5 mA emission current (75 W).

of alumina on PN polymerization, we performed FTIR, DSC, and rheological studies on alumina-filled samples without APB added.

Polymerization Catalysis. Different loadings of alumina were added to PN without APB in test tubes and immersed in an oil bath of 230 °C for curing. Samples were taken out at various time intervals for FTIR analysis to investigate the role of alumina in PN polymerization. Figure 5a shows the FTIR spectrum of 30A without APB over time and Figure 5b shows the appearance of triazine peak over time for PN, 10A, 20A, and 30A without APB. FTIR spectrum of PN, 10A, and 20A without APB over 3 h of curing are shown in Figure S5.

As seen in Figure 5a, the absorption peaks (1524 and 1359 cm^{-1}) corresponding to triazine ring were formed 30 min into the curing process of 30A even in the absence of curing agent APB. The IR absorption peak at 1600 cm^{-1}, attributed to aromatic structure vibration, was selected as the reference band to calculate the appearance of triazine peak over time in all the samples, as shown in Figure 5b. Since FTIR is a qualitative analysis, the time taken for the triazine peak appearance provides more information for PN polymerization catalysis than the absolute ratio value. Without curing agent APB and alumina, neat PN requires 3 h to form a triazine structure. However, with the addition of alumina in the absence of APB, triazine structures were formed more readily, proving that alumina has a catalytic effect on PN polymerization.

DSC. In addition, DSC analysis was conducted on alumina-filled PN samples without APB, and neat PN with and without

https://doi.org/10.1021/acsomega.2c02667
ACS Omega 2022, 7, 32996–33003

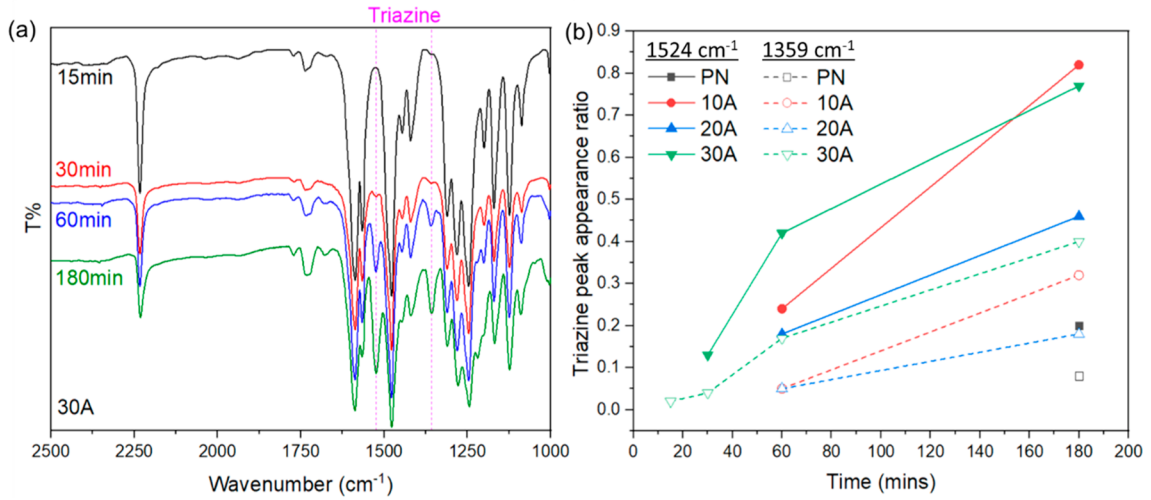

Figure 5. (a) FTIR spectrum of 30A without APB over time. (b) Appearance of the triazine peak over time for PN, 10A, 20A, and 30A with 1600 cm^{-1} as the reference band to calculate the ratio. FTIR spectra of PN, 10A, and 20A without APB over time can be found in Figure S5.

APB for comparison. Figure 6 shows the DSC curves of filler filled PN, focusing on the exothermic polymerization peak of

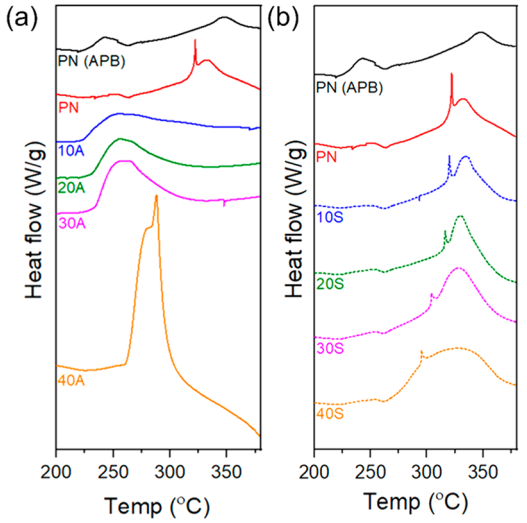

Figure 6. DSC curves of neat PN with and without APB and (a) alumina-filled PN without APB; (b) silica-filled PN without APB for the temperature range of 200−380 °C. Full spectra shown in Figure S6.

PN. An obvious reduction in the exothermic polymerization peak temperature was observed across all the alumina-filled PN as shown in Figure 6a. When 2.5 mol % of APB was added as a catalyst for PN polymerization, there is a small exothermic peak around 250 °C and another exothermic peak at 350 °C. Compared with neat PN without APB, the peak at 350 °C should be the original polymerization of PN and the one at 250 °C is due to the presence of APB catalyst.

The catalytic polymerization effect of PN due to alumina is observed from the thermal analysis of alumina-filled PN without APB in the DSC. As seen from Figure 6a, when alumina was added, an exothermic peak appears slightly above 250 °C, which is absent in neat PN without APB. Even though the exothermic peak corresponding to catalytic polymerization due to alumina is observed, it is likely to be less effective than the real catalyst such as APB since APB was only added in extremely small amounts. However, this is an important phenomenon, as it enhances the use of alumina in alumina-PN composites. This phenomenon is only observed in the alumina-filled PN samples; Figure 6b shows the silica filled PN and the exothermic peak corresponding to catalytic polymerization around 250 °C is absent across all silica loadings. The proposed mechanism, as illustrated in Scheme 2,

Scheme 2. Proposed Mechanism of Alumina-Catalyzed Polymerization

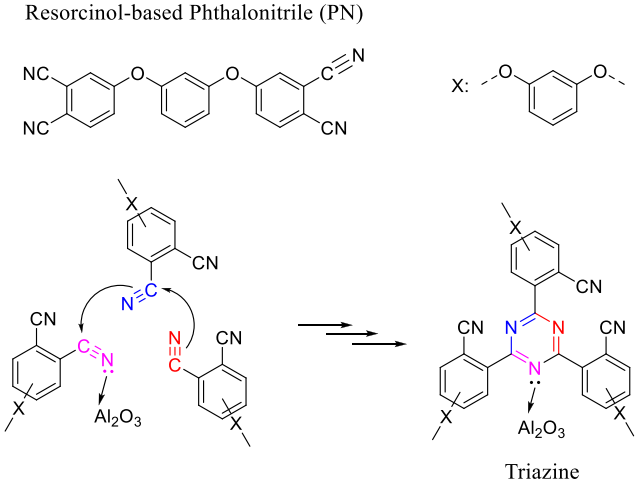

is that the alumina fillers form coordinate bonds with the nitrogen in the nitrile groups, hence weakening the nitrile bonds to allow triazine to form more readily. This mechanism is further supported by Figure 5b, which demonstrates that with the addition of alumina, triazine groups were detected much earlier in the polymerization process.

Rheological Studies. Neat PN and alumina-filled PN without APB were subjected to *in situ* curing and rheological studies at 250 °C in a rheometer to determine the time taken for cross-linked networks to be formed as an indication for effective polymerization that occurred. The time was taken when the storage modulus intersects with the loss modulus.

https://doi.org/10.1021/acsomega.2c02667
ACS Omega 2022, 7, 32996−33003

Table 2 summarizes the time taken for PN polymerization in the different samples without APB.

Table 2. Summary of Time Taken for Formation of Crosslinked Networks of Various PN Samples without APB

sample at 250 °C	time taken for cross-linked network
PN	47h 9m 14s
5A	77h 19m 43s
10A	58h 50m 29s
20A	3h 13m 50s
30A	5m 31s

As shown in Table 2, there is an increase in polymerization time at low loadings such as 5 and 10 wt %, and this could most probably be due to steric effects that are more prominent than catalytic effect. However, with further addition of alumina, the general trend is a decrease in the time taken for polymerization to occur. This further supports the catalytic polymerization brought about by alumina as shown in FTIR and DSC analysis previously.

The optimal addition of alumina can give rise to both catalytic polymerization of PN and improvement to other properties of alumina-PN composites such as coefficient of thermal expansion (CTE) and thermal stability. Figure 7 shows

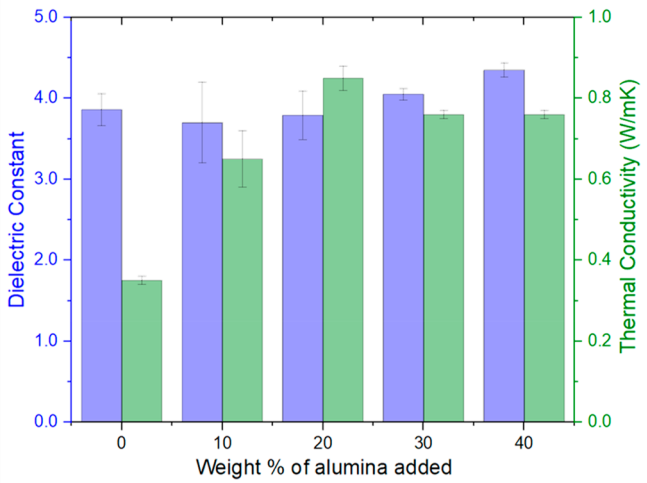

Figure 7. Dielectric constant and thermal conductivity of PN samples with various alumina loadings.

the increase in dielectric constant and enhanced thermal conductivity at 300 °C for alumina-filled PN. The approximate thermal conductivity of thermoset polymers is typically at 0.3 W/mK, the neat PN thermal conductivity at 300 °C is about 0.35 W/mK and addition of alumina results in an enhanced thermal conductivity at the same temperature. The thermal conductivity increased by 2-fold for 20 wt % alumina filler addition.

CONCLUSION

This work has demonstrated that the alumina particles not only act as fillers, but as a catalyst for polymerization of PN. The bonding interaction between alumina fillers and PN is confirmed to be chemical in nature through a combination of various characterization techniques. FTIR and XPS results indicate the presence of Al−N bonds between alumina fillers and PN and the catalytic polymerization effect is distinctly shown in DSC curves across the different alumina loaded samples. This finding is beneficial for the reduction of PN curing time without compromising crucial mechanical and thermal properties in order to make PN more applicable in various technologies.

ASSOCIATED CONTENT

Supporting Information

The Supporting Information is available free of charge at https://pubs.acs.org/doi/10.1021/acsomega.2c02667.

TGA of different weight percentages of silica-filled PN; chemical structure of PN and its polymeric forms, N 1s spectrum of postcured PN with APB added, NMR of PN monomer; SEM image and XPS of neat alumina fillers; summary table of the area ratio in N 1s XPS spectra of 50A and 70A samples collected with different emission current for comparison; XPS spectra of respective elements in 30 wt % SiO_2-filled PN before heat treatment and after postcuring; FTIR spectra of 0, 10, 30 wt % alumina-filled PN without APB over 3 h of curing time in an oil bath of 230 °C; DSC curves of filler-filled PN without APB in comparison with neat PN with and without APB catalyst (PDF)

AUTHOR INFORMATION

Corresponding Author

Chee Lip Gan − *School of Materials Science and Engineering, Nanyang Technological University, Singapore 639798, Singapore;* orcid.org/0000-0002-8420-3168; Email: clgan@ntu.edu.sg

Authors

Yu Shan Tay − *Rolls-Royce@NTU Corporate Laboratory, Nanyang Technological University, Singapore 637460;* orcid.org/0000-0002-1603-5318

Eric Jian Rong Phua − *School of Materials Science and Engineering, Nanyang Technological University, Singapore 639798, Singapore;* orcid.org/0000-0003-4263-3335

Zhong Chen − *School of Materials Science and Engineering, Nanyang Technological University, Singapore 639798, Singapore;* orcid.org/0000-0001-7518-1414

Complete contact information is available at: https://pubs.acs.org/10.1021/acsomega.2c02667

Author Contributions

†Y.S.T. and E.J.R.P. contributed equally to this work.

Notes

The authors declare no competing financial interest.

ACKNOWLEDGMENTS

This study is supported under the RIE2020 Industry Alignment Fund−Industry Collaboration Projects (IAF-ICP) Funding Initiative, as well as cash and an in-kind contribution from Rolls-Royce Singapore Pte Ltd. We acknowledge the Facility for Analysis, Characterisation, Testing and Simulation, Nanyang Technological University, Singapore, for use of their electron microscopy/X-ray facilities. We also acknowledge Vincent Gill for helpful input during technical discussion.

https://doi.org/10.1021/acsomega.2c02667
ACS Omega 2022, 7, 32996−33003

REFERENCES

(1) Dominguez, D. D.; Keller, T. M. Low-melting phthalonitrile oligomers: preparation, polymerization and polymer properties. *High Perform. Polym.* **2006**, *18* (3), 283−304.

(2) Lv, D.; Dayo, A. Q.; Wang, A. R.; Kiran, S.; Xu, Y. L.; Song, S.; Liu, W. b.; Wang, J.; Gao, B. C. Curing behavior and properties of benzoxazine-co-self-promoted phthalonitrile polymers. *J. Appl. Polym. Sci.* **2018**, *135* (31), 46578. Zhang, Z.; Li, Z.; Zhou, H.; Lin, X.; Zhao, T.; Zhang, M.; Xu, C. Self-catalyzed silicon-containing phthalonitrile resins with low melting point, excellent solubility and thermal stability. *J. Appl. Polym. Sci.* **2014**, *131* (20), DOI: 10.1002/app.40919. Guo, H.; Chen, Z.; Zhang, J.; Yang, X.; Zhao, R.; Liu, X. Self-promoted curing phthalonitrile with high glass transition temperature for advanced composites. *J. Polym. Res.* **2012**, *19* (7), 9918.

(3) Zeng, K.; Yang, G. Phthalonitrile matrix resins and composites. *Wiley Encycl. Compos.* **2011**, 1−14. Singh, A. S.; Shukla, S. K.; Pandey, A. K.; Tripathi, D.; Prasad, N. E. Synthesis and evaluation of catalytic curing behavior of novel nitrile-functionalized benzoxazine for phthalonitrile resins. *Polym. Bull.* **2018**, *75* (8), 3781−3800.

(4) Cao, X.; Vassen, R.; Stöver, D. Ceramic materials for thermal barrier coatings. *J. Eur. Ceram. Soc.* **2004**, *24* (1), 1−10.

(5) Derradji, M.; Wang, J.; Liu, W.-b. High performance ceramic-based phthalonitrile micro and nanocomposites. *Mater. Lett.* **2016**, *182*, 380−385.

(6) Derradji, M.; Ramdani, N.; Zhang, T.; Wang, J.; Feng, T.-t.; Wang, H.; Liu, W.-b. Mechanical and thermal properties of phthalonitrile resin reinforced with silicon carbide particles. *Mater. Des.* **2015**, *71*, 48−55.

(7) Derradji, M.; Ramdani, N.; Zhang, T.; Wang, J.; Lin, Z.-w.; Yang, M.; Xu, X.-d.; Liu, W.-b. High thermal and thermomechanical properties obtained by reinforcing a bisphenol-A based phthalonitrile resin with silicon nitride nanoparticles. *Mater. Lett.* **2015**, *149*, 81−84. Yang, X.; Li, K.; Xu, M.; Liu, X. Significant improvement of thermal oxidative mechanical properties in phthalonitrile GFRP composites by introducing microsilica as complementary reinforcement. *Composites, Part B* **2018**, *155*, 425−430. Derradji, M.; Ramdani, N.; Zhang, T.; Wang, J.; Gong, L.-d.; Xu, X.-d.; Lin, Z.-w.; Henniche, A.; Rahoma, H.; Liu, W.-b. Effect of silane surface modified titania nanoparticles on the thermal, mechanical, and corrosion protective properties of a bisphenol-A based phthalonitrile resin. *Prog. Org. Coat.* **2016**, *90*, 34−43.

(8) Derradji, M.; Ramdani, N.; Zhang, T.; Wang, J.; Gong, L. d.; Xu, X. d.; Lin, Z. w.; Henniche, A.; Rahoma, H.; Liu, W. b. Thermal and mechanical properties enhancements obtained by reinforcing a bisphenol-a based phthalonitrile resin with silane surface-modified alumina nanoparticles. *Polym. Compos.* **2017**, *38* (8), 1549−1558.

(9) Shan, S.; Chen, X.; Xi, Z.; Yu, X.; Qu, X.; Zhang, Q. The effect of nitrile-functionalized nano-aluminum oxide on the thermomechanical properties and toughness of phthalonitrile resin. *High Perform. Polym.* **2017**, *29* (1), 113−123.

(10) Gleiter, H. Nanostructured materials: basic concepts and microstructure. *Acta Mater.* **2000**, *48* (1), 1−29. Zunjarrao, S. C.; Singh, R. P. Characterization of the fracture behavior of epoxy reinforced with nanometer and micrometer sized aluminum particles. *Compos. Sci. Technol.* **2006**, *66* (13), 2296−2305.

(11) Ramdani, N.; Wang, J.; Wang, H.; Feng, T.-t.; Derradji, M.; Liu, W.-b. Mechanical and thermal properties of silicon nitride reinforced polybenzoxazine nanocomposites. *Compos. Sci. Technol.* **2014**, *105*, 73−79.

(12) Dueramae, I.; Jubsilp, C.; Takeichi, T.; Rimdusit, S. Thermal degradation mechanism of highly filled nano-SiO 2 and polybenzoxazine. *J. Therm. Anal. Calorim.* **2014**, *116* (1), 435−446.

(13) Phua, E. J. R.; Liu, M.; Cho, B.; Liu, Q.; Amini, S.; Hu, X.; Gan, C. L. Novel high temperature polymeric encapsulation material for extreme environment electronics packaging. *Mater. Des.* **2018**, *141*, 202−209.

(14) Tay, Y. S.; Phua, J. R. E.; Gan, C. L. Behavior of Resorcinol Based Phthalonitrile as High Temperature Encapsulant. In *2019 IEEE 21st Electronics Packaging Technology Conference (EPTC)*; IEEE: Piscataway, NJ, 2019; pp 711−715.

(15) Balogh-Hergovich, É.; Speier, G.; Réglier, M.; Giorgi, M.; Kuzmann, E.; Vértes, A. Synthesis, structure and spectral properties of a novel stable homoleptic iron (II) complex of 1, 3-bis (2′-pyridylimino) isoindoline, Fe (ind) 2. *Inorg. Chem. Commun.* **2005**, *8* (5), 457−459.

(16) Ji, S.; Yuan, P.; Hu, J.; Sun, R.; Zeng, K.; Yang, G. A novel curing agent for phthalonitrile monomers: curing behaviors and properties of the polymer network. *Polymer* **2016**, *84*, 365−370.

(17) Snow, A. W.; Griffith, J. R.; Marullo, N. Syntheses and characterization of heteroatom-bridged metal-free phthalocyanine network polymers and model compounds. *Macromolecules* **1984**, *17* (8), 1614−1624.

(18) Seoudi, R.; El-Bahy, G.; El Sayed, Z. FTIR, TGA and DC electrical conductivity studies of phthalocyanine and its complexes. *J. Mol. Struct.* **2005**, *753* (1−3), 119−126.

(19) Balasubramanian, C.; Bellucci, S.; Cinque, G.; Marcelli, A.; Guidi, M. C.; Piccinini, M.; Popov, A.; Soldatov, A.; Onorato, P. Characterization of aluminium nitride nanostructures by XANES and FTIR spectroscopies with synchrotron radiation. *J. Phys.: Condens. Matter* **2006**, *18* (33), S2095.

(20) Vanbuskirk, J. W.; Prokofyeva, T.; Seon, M.; Nikishin, S.; Temkin, H.; Holtz, M.; Zollner, S. FTIR and Raman Studies of the Vibration Modes in High Purity AlN Films Grown on Silicon. *Joint Fall Meetings of the Texas Section of the APS, AAPT, and Zone 13 of the SPS*; Austin, TX, October 28-30, 1999 ; American Physical Society: College Park, MD, 1999; F36.04.

(21) Fan, Q.; Luy, J.-N.; Liebold, M.; Greulich, K.; Zugermeier, M.; Sundermeyer, J.; Tonner, R.; Gottfried, J. M. Template-controlled on-surface synthesis of a lanthanide supernaphthalocyanine and its open-chain polycyanine counterpart. *Nat. Commun.* **2019**, *10* (1), 1−8.

(22) Dieckhoff, S.; Schlett, V.; Possart, W.; Hennemann, O.-D.; Günster, J.; Kempter, V. Characterization of triazine derivatives on silicon wafers studied by photoelectron spectroscopy (XPS, UPS) and metastable impact electron spectroscopy (MIES). *Appl. Surf. Sci.* **1996**, *103* (3), 221−229.

https://doi.org/10.1021/acsomega.2c02667
ACS Omega 2022, 7, 32996−33003